

# Energy Consumption Estimation in Lap Time Simulation

José Filipe Dias Duque Marques Loureiro  
jfilipeddmloureiro@tecnico.ulisboa.pt

Instituto Superior Técnico, Universidade de Lisboa, Lisboa, Portugal

June 2018

## Abstract

A big challenge in the design of a battery electric vehicle is the mileage. Batteries can make up to a significant part of the vehicle's weight and so they must be properly designed for the minimum storage needed. This paper aims to implement energy consumption estimation in a Lap Time Simulator (LTS) for motorsport vehicles and to understand how the complexity of the vehicle model affects the simulation and estimation results. A LMP3 category prototype racing car is parametrized in two Quasi-Steady-State simulators. One is a commercial software composed of a 4-wheel vehicle model. The second was developed in the scope of this work as a simpler alternative composed of a Point-Mass model. This paper details the decision making behind the development of a Quasi-Steady-State simulator and the simplifications made in the Point-Mass model. Data was collected in a test day at *Autódromo do Estoril* with the best lap serving as validation for both simulators. A sensitivity analysis is done to parameters of the Point-Mass model to validate its utility. The results with the experimental data show that the less complex and much easier to implement Point-Mass model has satisfactory results when compared to the 4-wheel model, calculating lap time with 7% error. Therefore, a simple and easy to implement vehicle model can be applied to LTS to estimate energy consumption in motorsport vehicles. The bigger source of discrepancies lies on the simplification in the tyres model.

**Keywords:** Motorsport, Energy Consumption, Quasi-Steady-State, Point-Mass, Simulation

## 1. Introduction

Motorsport is used as the benchmark for testing new technologies for the automotive industry. The goal of any motorsport event is to complete a certain distance of a pre-defined path in the minimum time possible in a motoring vehicle. Racing tests the vehicle's limits of performance and allows to gain empiric knowledge about the components designed to a car or motorcycle that can be put into a production vehicle to be sold for the general public.

Ideally, within a certain regulation, a racing car will have adjustable parameters to make it more efficient in different venues and so the right set-up must be discovered. In the present times, most championships have restrictions in extra tests outside of a racing weekend to lower the budget needed to compete. Simulation of competition vehicles comes to suppress the need to know how the variation of set-up parameters translate to on-track behaviour with limited testing. This way, simulation accelerates the development of a vehicle either by giving initial inputs to design or to short cut the process of testing.

This paper objective is to understand if energy consumption estimations can be made through a Lap Time Simulator (LTS), how complex should the vehicle model be and what are the parameters that influence the simulated energy consumption the most.

A Lap Time Simulator is a tool in vehicle design applied to motorsport. The goal of such tool is to find the best possible lap time of a certain vehicle in a certain track and understand how the variation of some of it's parameters influence this lap time. Siegler [1] describes a LTS as a vehicle handling model that connects many different manoeuvres all performed at the limit of the vehicle. The vehicle is simulated to be at it's limit at all points of a track: maximum lateral acceleration in corners and maximum longitudinal acceleration in straights, thus the best possible lap time.

The first approach to lap time simulation consisted of individual hand-made calculations for certain sectors of the track and summing the resulting sector times to get the predicted lap time. Equations of motion were hand derived and increasingly solved by digital computers until the 1980's. In

1971, the first example of a g-g diagram was published, making way to the development of quasi-steady-state simulations. Milliken improved the quasi-steady-state simulations using the "bicycle" model [2].

From a planar dynamics point of view, when a vehicle is turning there is yaw movement (rotation about the vertical axis), described by equations of motion that account the forces generated at the tyres. Simulators differ in the way they solve these equations of motion. A cornering vehicle is said to be in equilibrium when the sum of yaw moment around the CG is null and the rate of rotation is constant. This is the steady-state condition that happens at the apex of a corner.

Neves [3] explains, by the equations of non-uniform circular motion, that when describing a corner with longitudinal (x-axis or tangent to motion) acceleration different from zero, the yaw acceleration will also be non-zero. Nevertheless these accelerations can be constant, defining the idea of Quasi-Steady-State (QSS). This is the condition when the car has more than one constant acceleration:  $a_x$  and  $a_y$  are both non-zero and constant at the same time, meaning that the vehicle is cornering but its velocity is changing. In QSS the car is said to be momentarily in static-equilibrium.

Simulators can vary in the type of the above stated conditions (Steady-State, Quasi-Steady-State, Transient) it simulates the car but also in the type of vehicle model used. Concerning the vehicle model, the simpler type is the point-mass, a single point with mass that represents the whole car with 2 degrees-of-freedom (DOF): longitudinal and lateral. Milliken [2] introduced the more advanced "bicycle" model where the two front tyres, like the rear ones, are combined in one and the car is simulated as standing on two different tyres, making a distinction between front and rear. Four-wheel models are an improvement to the "bicycle" model that can estimate more accurately the slip angles at each wheel individually and simulate both longitudinal and lateral weight transfer through suspension mechanics and kinematics calculations as well as distinguishing sprung and unsprung masses.

In this work the calculations of energy consumption correspond to the Battery-to-Wheel portion of a vehicle's Life Cycle Assessment: the energy required at the wheels to drive the vehicle [4] [5]. To drive a body with constant acceleration there must be an equilibrium of forces acting on said body. For a road vehicle this corresponds to an equilibrium between the wheels and the road at the contact patch of the tyres and a total resistance to the movement of the vehicle [6]. This force balance corresponds to equation (1).

$$F = m g (f_{rr} \cos(\zeta) + \sin(\zeta)) + \frac{1}{2} \rho C_D A_f v^2 + (m + m_f) a \quad (1)$$

where  $m$  is the vehicle's total mass,  $g$  is the gravitational acceleration,  $f_{rr}$  is the tyre's rolling resistance coefficient,  $\zeta$  is the road inclination angle,  $\rho$  is the air density,  $C_D$  is the aerodynamic drag coefficient of the vehicle,  $A_f$  is the vehicle's frontal area,  $m_f$  is the fictive mass of rolling inertia,  $v$  is the velocity and  $a$  is acceleration. When travelling a distance  $d$  this force translates to energy and this will be the amount drawn from the battery of an electric vehicle, given by equation (2).

$$E = [m g (f_{rr} \cos(\zeta) + \sin(\zeta)) + \frac{1}{2} \rho C_D A_f v^2 + (m + m_f) a] d \quad (2)$$

Literature review revealed models computed and optimized to predict Battery-to-Wheel consumption for specific electric powered vehicles using data from experiments and equation (2) but all of them are specific to a car and need real data from testing. Because of this they are not suitable for other vehicles either they have been tested or not.

This first section introduces the motivation and objective of this work. Here is also presented the state of the art regarding Lap Time Simulators and energy consumption estimation of electric vehicles. On Section 2, the two simulators used (PMSim and RaceLap) are presented. PMSim was developed in the scope of this work and thus a more thorough explanation on the Point-Mass vehicle model is made as well as describing the approach made to Quasi-Steady-State simulation. Section 3 shows the experimental data used for validation and presents the simulation outputs from both simulators used. Also in this section, a sensitivity analysis is done to PMSim and the energy consumption estimator implemented. Finally, in the last section are stated the conclusions of this work.

## 2. Implemented Simulations

In an LTS a race track is discretized in segments. The lap time is calculated by summing all the individual segment times, i.e., how long it takes the vehicle from entering to exiting each segment. The main distinctions between simulators can be the simulation type (Steady-State, Quasi-Steady-State, Transient) and the vehicle model (Point-Mass, "Bicycle", 4-Wheel).

### 2.1. Point-Mass Vehicle Model

In this model the whole vehicle sums up to a point that can be said to be supported on one

tyre. The longitudinal or lateral force produced by this tyre is a consequence of the vertical load ( $F_z$ ) exerted on it - the point's weight plus the down force generated while moving. Being the simpler method to parametrize a vehicle, the Point Mass is the model that requires the least parameters.

Here, tyres are simplified to only two parameters defining the longitudinal and lateral coefficients of friction:  $\mu_x$  and  $\mu_y$ , respectively. The forces generated at the tyres are given by equations (3).

$$F_x = \mu_x F_z \quad (3a)$$

$$F_y = \mu_y F_z \quad (3b)$$

The friction coefficients can be estimated using equations (4) of the Pacejka [7] *Magic Formula Tyre Model* resorting to only 5 out of 89 coefficients of the complete model - *Pacejka 2002*.

$$\mu_x = (p_{Dx1} + p_{Dx2} df_z) \lambda_{\mu x}^* \quad (4a)$$

$$\mu_y = (p_{Dy1} + p_{Dy2} df_z) / (1 + p_{Dy3} \gamma^{*2}) \lambda_{\mu y}^* \quad (4b)$$

where  $p_{Dx1}$ ,  $p_{Dx2}$ ,  $p_{Dy1}$ ,  $p_{Dy2}$  and  $p_{Dy3}$  are coefficients of the *Pacejka 2002 Tyre Model* and  $df_z$ ,  $\gamma^*$ ,  $\lambda_{\mu x}^*$  and  $\lambda_{\mu y}^*$  are parameters of the same model.

The model of the powertrain system consists of the engine torque curve, the gear ratios of the gearbox and the final reduction at the differential. The propulsion force generated by the engine is function of the power produced which in turn is a function of torque and so the engine limitation depends on where in the motor curves the vehicle is operating. It is also needed to simulate when to change gear, i. e., what gear should be engaged at every point of the track. To achieve this it is assumed that the gear selected is the one that makes the engine produce more power for a certain linear velocity of the vehicle and thus producing the most propulsion force of the whole set of gears. The powertrain simulation is given by equations (5).

$$\omega_j = \frac{gr_j diff v}{r_w} \quad (5a)$$

$$\omega_{jrpm} = \frac{\omega_j 60}{2\pi} \quad (5b)$$

$$P_j = T_j \omega_j \quad (5c)$$

$$F_e = \frac{\max(P_j)}{v} \quad (5d)$$

where  $j$  is the gear index,  $\omega$  is the engine angular speed in rad/s,  $\omega_{jrpm}$  is the engine angular speed in rpm,  $gr$  is a gear ratio,  $diff$  is the differential final ratio,  $v$  is the vehicle's linear velocity,  $r_w$  is the wheel radius,  $P$  is power,  $T$  is torque and  $F_e$  is the resulting propulsion force.

The aerodynamics in this model sum up to equations (6) with the influence of constant drag and lift coefficients.

$$F_D = \frac{1}{2} \rho C_D A_f v^2 \quad (6a)$$

$$F_L = \frac{1}{2} \rho C_L A_f v^2 \quad (6b)$$

where  $\rho$  is the air density,  $C_D$  and  $C_L$  are the drag and lift coefficients, respectively,  $A_f$  is the vehicle's frontal area and  $F_D$  and  $F_L$  are the drag and lift (or downforce) forces, respectively.

## 2.2. Steady-State Simulation

The car is said to be in a steady-state condition when it has a constant acceleration and, in the case of a corner, constant radius as well. This is the most simple approach to lap time simulation. Given that a race track is composed of straights and various types of turns, the steady state condition is simulated in each segment of the track, i.e., acceleration is constant in each segment. Figure 1 illustrates the entering velocity, acceleration and exit velocity within each segment.

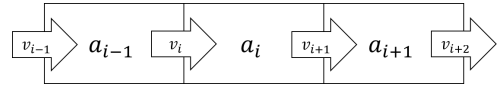


Figure 1: Three track segments

In order to know where the braking point is when approaching each turn, the simulation is divided into two phases, the Forward and Reverse simulations, as in [8]. In the forward simulation only positive acceleration occurs: the velocity increases in a straight line until a corner segment appears where it will be set for the maximum corner velocity. The reverse simulation does the same but in the opposite way of the circuit, with the forces moving the car being tyres braking force, drag force and the tyre's rolling resistance, all in the same direction. The final velocity profile of the car on a given track is the minimum of the two simulations (Forward and Reverse) in each segment, as shown in Figure 2.

Each segment will have an entering velocity, exit velocity and constant acceleration, as shown in Figure 1. Denoting  $i$  as the current segment, its entering velocity is

$$v_i = v_{i-1} + a_{i-1} \Delta t_{i-1} \quad (7)$$

where  $t_{i-1}$  is the time that took to travel the previous segment. The longitudinal acceleration of the segment  $i$  is also dependent of the entering velocity  $v_i$  and is calculated using equations (3), (5) and (6). The process to calculate  $a_x$  in the segment  $i$  for the forward simulation stage is:

$$F_z = m g + F_L \quad (8a)$$

$$F_e = \frac{P}{v_i} \quad (8b)$$

$$F_{rr} = f_{rr} F_z \quad (8c)$$

$$F_{tx} = \mu_x F_z \quad (8d)$$

$$a_{x_i} = \frac{\min(F_{tx}, F_e) - F_D - F_{rr}}{m} \quad (8e)$$

where  $m$  is the vehicle's mass,  $g$  is the gravitational acceleration,  $f_{rr}$  is the tyre's rolling resistance coefficient and  $F_{rr}$  is the rolling resistance force. In the case of a corner segment, the maximum corner velocity must be computed. Taking into account only the lateral acceleration:

$$a_{y_i} = \frac{v_i^2}{r_c} \leftrightarrow v_i = \sqrt{a_{y_i} r_c} \quad (9)$$

where  $r_c$  is the corner radius. From equation (9) is seen that the velocity in a corner segment is a function of lateral acceleration. Nevertheless, the opposite is also true and so:  $v_i(a_{y_i})$  and  $a_{y_i}(v_i)$ . To solve this problem an iteration must be done.

The iteration process to compute the maximum corner velocity uses the following equations in the given order, starting with  $v_i = 0$ , until some stopping criteria is met:

$$F_L = \frac{1}{2} \rho C_L A_f v_i^2 \quad (10a)$$

$$F_z = w + F_L \quad (10b)$$

$$F_{ty} = \mu_y F_z \quad (10c)$$

$$a_{y_i} = \frac{F_{ty}}{m} \quad (10d)$$

$$v_i = \sqrt{a_{y_i} r_c} \quad (10e)$$

where  $F_{ty}$  is the lateral force generated by the tyres. In this work, the stopping criteria chosen was the result of an exponential moving average of the  $v_i$  values after 300 iterations. This method helps to find a converging value for cases where the iteration oscillates indefinitely.

The time that takes to travel through a segment is

$$\Delta t_i = \frac{d_i}{v_i} \quad (11)$$

where  $d_i$  is the length of the segment.

In the reverse simulation stage, the calculations start from the same point as the Forward simulation but go in the opposite direction of the track. Here the engine propulsion force is not considered and the longitudinal acceleration is given by:

$$a_{x_i}^{rev} = \frac{F_{tx} + F_D + F_{rr}}{m} \quad (12)$$

The method to compute the maximum corner velocity is the same, given that the cornering is only dependent on the tyre capacity to produce lateral force.

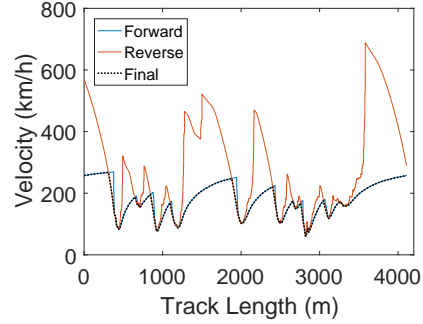


Figure 2: Velocity profiles from Forward and Reverse Simulations. Resulting lap velocity profile in dotted black.

### 2.3. Quasi-Steady-State Simulation

Analysing the tyre, one knows that it can produce a certain longitudinal force at a given vertical load (which depends on the velocity) and the same for the lateral force. In the case of the Point Mass Model, these forces are given by equations (3). If one considers that  $F_x$  and  $F_y$  in those equations are the maximum forces the tyre can produce in a pure longitudinal or lateral case, respectively, one can assume that if when describing a certain corner the driver is not making the car turn at the limit of the tyre capability -  $F_y^{max}$  - there is still some longitudinal force to be produced.

Every corner segment has a maximum velocity to be driven by a certain car fitted with certain tyres and this velocity is known from the maximum  $F_y$  the tyre can produce in that car. Not being at the limit of the tyre capability means the entering velocity of that segment is not the maximum velocity and so the tyre can still generate a certain amount of longitudinal force to make the car reach the maximum corner velocity. The amount of longitudinal force that can still be generated is given by an ellipse equation:

$$\left( \frac{F_{tx}}{F_{tx}^{max}} \right)^2 + \left( \frac{F_y}{F_y^{max}} \right)^2 = 1 \quad (13)$$

$$\leftrightarrow F_{tx} = \sqrt{1 - \left( \frac{F_y}{F_y^{max}} \right)^2} \cdot F_{tx}^{max}$$

This is the case for both Forward and Reverse simulations, the difference being that in the Forward case,  $F_x = \min(F_e, F_{tx})$  and in the reverse case  $F_x = F_{tx}$ .

Figure 3 shows the result of applying equation (13) to  $F_y \in [0; F_y^{max}]$  for a specific velocity. This

is a g-g diagram, a plot of  $a_x$  vs  $a_y$  that quantifies the vehicle's maximum accelerations capability. This diagram changes for each value of velocity and only one half of it is computed and plotted because it is symmetrical for symmetrical cars. Negative  $a_x$  values denote longitudinal acceleration for braking. The saturation at the top, for positive  $a_x$ , is a result of the engine propulsion force being the limiting factor, i. e., in these points:  $F_e < F_{tx}$ . A g-g diagram can be used as a tool to measure vehicle performance and behaviour.

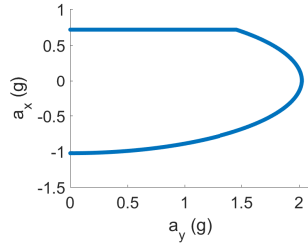


Figure 3: Example of a g-g Diagram for AD03 at 40m/s

The iteration process to find the maximum corner velocity remains the same, given that this is only a function of  $F_y^{max}$ .

#### 2.4. RaceLap Simulator

RaceLap is a Quasi-Steady-State simulator that uses a 4-wheel vehicle model coded in Matlab. This software calculates the forces acting on the car that give an equilibrium of movement based on 5 degrees of freedom:

- Suspended mass equilibrium in roll - roll angle;
- Suspended mass equilibrium in pitch - pitch angle;
- Suspended mass vertical equilibrium - CG height;
- Lateral equilibrium of the whole vehicle - steering rack position;
- Equilibrium of the whole vehicle in yaw - sideslip angle.

Differing from the approach in section 2.3, the g-g diagrams in RaceLap are computed through iteration, instead of a simple ellipse equation. Before solving the five equations of motion the simulator calculates the forces and displacements acting on various modules of the car: Aerodynamic, Suspensions, Tyres and Powertrain. An iterative algorithm then solves the 5 general equations and the lateral acceleration limit is found for each segment. This

process is done for both the forward and reverse phases of simulation.

On the other hand the velocity calculations are done the same way as described in section 2.2, with the final velocity profile being the corresponding minimum of the forward and reverse velocities in each sample.

### 3. Results

Here are presented the outputs of both simulators used: the Point-Mass simulator developed (PMSim) and RaceLap, the simulator available at Adess-AG. PMSim is a Quasi-Steady-State simulator that implements the vehicle model presented in Section 2.1 using 11 parameters while for RaceLap a comprehensive and detailed list of 94 parameters is needed. This means the two compared simulators have very different complexities.

The validation for simulation comes from the results of a test day that an AD03 did at *Autódromo do Estoril* (Estoril). The best lap (1:38.295 (min:sec)) velocity profile is used as reference to compare the simulation results. In simulations, the vehicle was parametrized to approximate the real car set-up configuration.

The main difference from the real to simulated vehicle lies on the front tyres. Despite being the correct model, the parametrized front tyres do not correspond to the real compound used. LMP3 category cars usually race medium compound tyres at the front and hard at the rear but the manufacturer only provides the Pacejka model of the hard compound. This means that the simulated grip from the front tyres does not correspond to the real ones. For this reason, an adjustment of the grip level of the front tyres was added in order to achieve the minimum corner velocities verified in the real lap. It is also to be noted that the real lap trajectory was 100 meters shorter than the track used in simulation.

Regarding energy consumption in the test day, not only in the fastest lap but also in all laps done in the same pace (1:38's an 1:39's) the fuel consumption registered was of 2 litres/lap. The conversion from litres to kWh will be assumed the same as presented in [9] where the energy density is considered 9.6111 kWh/litre. Using this conversion, the real energy consumption for a lap of the Estoril track is 19.22 kWh.

#### 3.1. RaceLap

Finally are presented the final main results from the RaceLap simulation in Figure 4.

Despite always achieving higher velocities, the simulation gives a slower time. This can be justified by the extra 100 meters of the trajectory simulated. Taking the mean of the RaceLap velocity, 46.59 m/s, the extra 100 meters account for an ex-

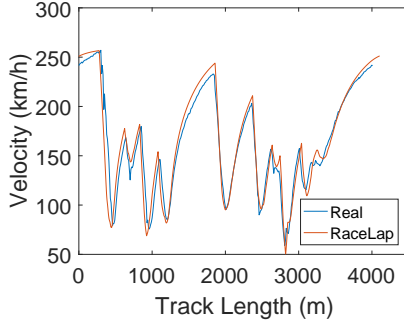


Figure 4: Velocity profiles of both RaceLap simulation (1:39.588) and the real lap (1:38.295).

tra 2.146 seconds, giving a lap time prediction of 1:37.442 for the same trajectory that was done in the best lap of the real test. This result is given in Table 1 under "Predicted real trajectory time". The top speed registered in the real lap was 257 km/h, with the simulation giving 256.6 km/h. The main difference between the profiles is in the positive acceleration stages whereas in the braking stages the profiles are more similar.

Applying equation (2), the amount of energy needed to perform a lap as simulated in RaceLap is 5.62 kWh. Assuming 100% efficiency for an electric powertrain, this would be the calculated amount of energy consumed from a battery if AD03 was an electric vehicle. Because this energy actually comes from a combustion engine, this value has to be divided by the efficiency of the powertrain (tank-to-wheel). Advised by the engine manufacturer company, the engine efficiency is considered to be 30%. The gearbox must also be accounted for, in this case with an efficiency of 96.04%. The total energy consumption of the simulated lap is then

$$E = \frac{5.62}{0.3 \cdot 0.9604} = 19.51 \text{ kWh} \quad (14)$$

The resulting energy consumption calculated value is 73.18% from the linear inertia term, 24.52% from aerodynamic drag and 2.3% from tyres rolling resistance.

Table 1: RaceLap main results

	Real	RaceLap	Error(%)
Lap Time(min:sec)	1:38.295	1:39.588	1.32
Pred real trajec time <sup>1</sup> (min:sec)	-	1:37.442	-0.87
Avg Vel(km/h)	164.5	167.7	1.95
Top Vel(km/h)	257	256.6	-0.16
Enrg Cons(kWh)	19.22	19.51	1.5

<sup>1</sup>Prediction for the real trajectory by subtracting time corresponding to travelling 100 meters at the simulation average velocity from the simulation Lap Time.

### 3.2. PMSim

The final main results from the Point-Mass simulation are presented in Figure 5.

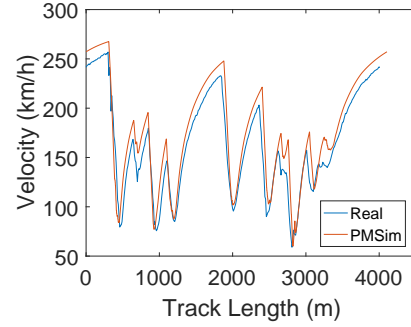


Figure 5: Velocity profiles of both Point-Mass simulation (1:31.507) and the real lap (1:38.295).

This model resulted in a more optimistic simulated vehicle behaviour. Even with the extra 100 meters in the simulation trajectory, the lap time is still considerably lower than the real case. This corresponds to a larger error than the RaceLap results with minimum corner velocities higher than the real case. PMSim's lower lap time is a consequence of higher top speeds in straights and a significant corner velocity difference in turns 2, 8, 11 and the entry of 13, like in the final RaceLap results. The average speed of 49.87 m/s gives a prediction of 1:29.502 for the real trajectory. This prediction, as explained in the previous section, corresponds to subtracting the time equivalent to travelling 100 meters at the average velocity of the simulation results and is given in Table 2 under "Predicted real trajectory time". The top speed is 267.6 km/h.

Regarding fuel consumption, equation (2) results in 6.62 kWh of required energy to complete a lap. As explained before, this value has to be divided by the powertrain efficiency that accounts for both the gearbox and the combustion engine.

$$E = \frac{6.62}{0.3 \cdot 0.9604} = 22.98 \text{ kWh} \quad (15)$$

The resulting energy consumption calculated value is 73.16% from the linear inertia term, 24.69% from aerodynamic drag and 2.15% from tyres rolling resistance.

Table 2: PMSim main results

	Real	PMSim	Error(%)
Lap Time(min:sec)	1:38.295	1:31.507	-6.9
Pred real trajec time <sup>2</sup> (min:sec)	-	1:29.502	-8.9
Avg Vel (km/h)	164.5	179.5	9.1
Top Vel (km/h)	257	267.6	4.1
Enrg Cons(kWh)	19.22	22.98	19.56

<sup>2</sup>Prediction for the real trajectory by subtracting time corresponding to travelling 100 meters at the simulation average velocity from the simulation Lap Time.



### 3.3. Point-Mass Sensitivity Analysis

In this section, PMSim is used to apply sensitivity analysis on parameters of the Point-Mass model. In the process, PMSim and RaceLap are compared through common outputs in both simulators. The sensitivity analysis gives insight into the utility of the Point-Mass model by changing input parameters different from the nominal used in section 3.2. Together, both the simulations outputs comparison and the sensitivity analysis done on the PMSim lead to conclusions regarding the complexities of the two vehicle models. The mentioned common outputs between both simulators are:  $a_x$ ,  $a_y$ ,  $F_z$ ,  $F_D$  and  $v$ . In Figure 6 is the comparison of the velocity profiles from both simulators discussed in sections 3.1 and 3.2.

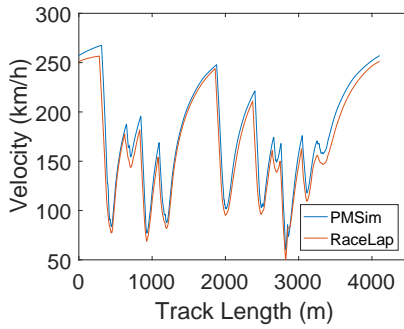


Figure 6: PMSim and RaceLap velocity profiles in a lap at Estoril.

The Point-Mass model results in an optimistic simulation in the sense that the overall lower lap time results from higher velocities in both corners (lateral behaviour) and straights (longitudinal behaviour). The sensitivity analysis will provide insight into what parameters most contribute to the error of PMSim and if the higher straight-line velocities are a consequence of high corner velocities or the two are independent of one another.

#### 3.3.1 Drag Force ( $F_D$ )

A Point-Mass model has a fixed value for  $SCX$  while on RaceLap, with a 4-wheel vehicle, this value varies with the front and rear ride heights as in reality. The default  $SCX$  value chosen for the PM model was the mean of this variation in RaceLap.

In Figure 7 is the variation of the drag force ( $F_D$ ) in RaceLap for one lap. The RaceLap velocity output was used to compute a  $F_D$  profile with constant  $SCX$  equal to the mean following equation (6a). The result shows that the profiles only diverge in the sections of the lap where the RaceLap  $SCX$  is lower than the mean constant value. These sections correspond to the 3 main straights, with the

difference being higher the longer the straight is.

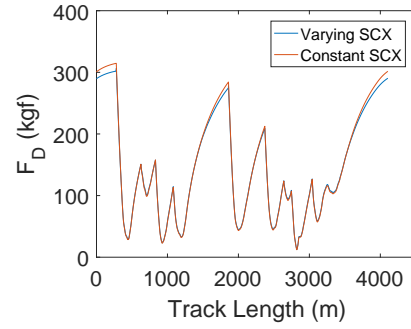


Figure 7: RaceLap  $F_D$  profile (blue) and equation (6a) applied for RaceLap velocity profile and constant  $SCX$  (orange).

Aerodynamic drag mainly affects the straight line speed. In order to see the influence of  $SCX$  on the overall lap performance, a sensitivity analysis was done to this coefficient. The results of lap time analysis make for a linear relation between the two variables with a slope of 0.4 s/0.1  $SCX$ . Even for very high  $SCX$ , the simulation lap time is still far lower than the real case, leading to the conclusion that the drag coefficient is not the parameter that causes the lower PMSim lap times. Analysing for top speed it is seen that this is not sensible enough to the  $SCX$ . Approximating the variation to a linear function, the rate of change is -5.25 km/h / 0.1  $SCX$ . Knowing that the maximum variation of  $SCX$  in RaceLap is 0.07, it is concluded that the nominal value used in the Point-Mass model is not the cause of simulation error in top speed.

#### 3.3.2 Longitudinal Acceleration ( $a_x$ )

In section 2 is discussed that the longitudinal acceleration can be limited either by the powertrain or the tyres longitudinal grip. For this reason, this section's analysis lies on a torque factor and on the tyre's longitudinal coefficient of friction  $\mu_x$ . Figure 8 shows the variation of  $a_x$  for both simulators in one lap. The main difference between both profiles is in the braking stages, with PMSim achieving higher negative acceleration.

**Torque Factor** As explained above, the higher top speeds can be a consequence of the real powertrain running conditions having a smaller efficiency than predicted. To evaluate this possibility, a sensitivity analysis was applied to a factor that impacts the engine performance. The torque output from the engine is multiplied by this factor in order to simulate either a powertrain lower efficiency or the throttle pedal not being actuated in full capacity.

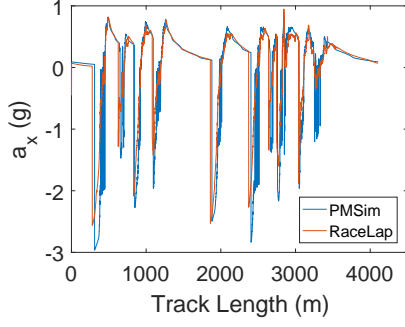


Figure 8: Longitudinal acceleration profile in RaceLap and PMSim.

It is observable that this factor has bigger impact in top speed. Because the corner speeds are maintained, the lap time is still far lower than the real case but the longitudinal behaviour is considerably affected. Considering a factor of 0.9, the lap time error lowers to 5.74%, average speed lowers to 7.04%, top speed lowers to 0.41% and energy consumption lowers to 2.85%.

**Longitudinal coefficient of friction ( $\mu_x$ )** The coefficient of friction is composed of two parameters that regulate it's linear relation with the vertical load exerted on the tyre ( $F_z$ ): the slope ( $m_x$ ) and the intercept ( $b_x$ ).

In the case of a simple straight line acceleration from zero the tyres are the limiting factor until the car achieves around 110 km/h. This means that  $\mu_x$  has a bigger impact at the exit of slow corners. The longitudinal coefficient of friction is also responsible for the braking capacity of the vehicle.

The simulation is more sensitive to  $b_x$  than  $m_x$  which is expected because the slope ( $m_x$ ) is 5 units of magnitude lower. The maximum decrease of the intercept value resulted in a lap time still considerably lower than the real case and a top speed of 266.191 km/h, corresponding to a decrease of 0.52 %. This leads to the conclusion that lowering the tyre longitudinal grip can contribute to more realistic lap times but not on it's own. The higher values of  $a_x$  in the braking stages are a consequence of modelling the longitudinal behaviour of the tyres through the friction coefficient but its impact in lap time is not enough to be considered a main source of error. Also concluded is that  $\mu_x$  has no significant impact on top speed, which is realistic.

### 3.3.3 Downforce ( $F_z$ )

Just as when discussed about drag, the downforce (or lift) coefficient,  $SCZ$ , changes with front and rear ride heights in a real vehicle and RaceLap replicates this. The mean value of the  $SCZ$

variation in RaceLap is also chosen as the nominal value in the Point-Mass model. Figure 9 presents the RaceLap  $F_z$  output and the profile generated from applying the aerodynamic downforce equation (6b) to the RaceLap velocity vector with constant  $SCZ$  equal to the nominal Point-Mass model value.

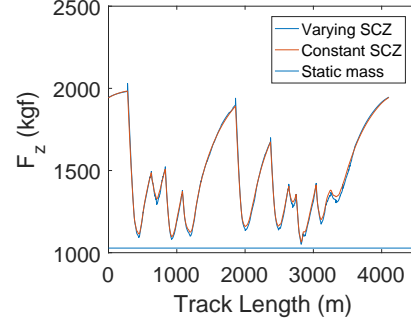


Figure 9: RaceLap  $F_z$  profile (blue) and equation (6b) applied for RaceLap velocity profile and constant  $SCZ$  (orange). AD03 static mass in horizontal line.

The points where there is a bigger difference in  $F_z$  between the two simulators correspond to where the  $SCZ$  coefficient in RaceLap is below the nominal value of the Point-Mass model. These points correspond to the corners of the track.

The lap time analysis showed an overall linear relation with  $SCZ$  with an approximate slope of -0.2 s/0.1  $SCZ$  which is lower than the LapTime( $SCX$ ) relation in module. The maximum decrease still holds a lap time far from the RaceLap result and the real case, leading to the conclusion that the  $SCZ$  nominal value used is also not the parameter mainly responsible for the error of simulation.

The main influence of the downforce is in corner velocity for it impacts the tyre grip. Recalling equation (4),  $F_z$  is the argument of both  $F_y$  and  $\mu_y$ . This directly impacts  $a_y$  and so this analysis must be done together with the results from section 3.3.4.

### 3.3.4 Lateral Acceleration ( $a_y$ )

The lateral acceleration of the vehicle resorts on the tyres lateral grip. From equation (3b) is known that the lateral force  $F_y$  the tyre produces is a linear function of the vertical force exerted on it - the downforce  $F_z$ . Figure 10 shows the comparison of the registered values of  $a_y$  in a lap in Estoril for both simulators.

It is evident that the higher corner velocities in PMSim are a consequence of higher lateral acceleration. This can have two causes: the downforce ( $SCZ$ ) or the friction ( $\mu_y$ ) coefficients. Sec-



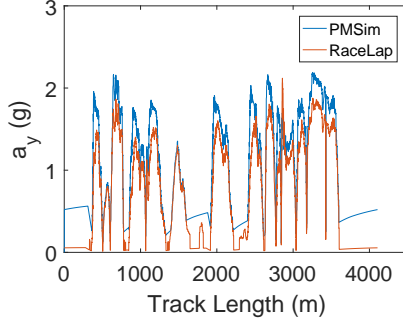


Figure 10: Lateral acceleration profile in RaceLap and PMSim.

tion 3.3.3 presents the sensitivity analysis applied to the  $SCZ$  coefficient. Regarding  $\mu_y$  is recalled equation (3b) that has two parameters:  $m$  and  $b$ . These are the slope and the intercept of the grip linear function, respectively, here mentioned as  $m_y$  and  $b_y$ . The sensitivity analysis to the tyres  $F_y$  is done on these two grip parameters.

Results show that the intercept is more sensitive than the slope. This is expected as the slope is 5 units of magnitude lower. This way, the intercept variation is more suitable to describe the sensitivity of the lateral friction coefficient  $\mu_y$ . A drop of 18.75% in  $b_y$  resulted in a 0.08% error in lap time. This result show that  $\mu_y$  is a very sensitive parameter and together with the analysis of Figure 10 is concluded that it is a major responsible for the bigger error of the Point-Mass simulation. The drop of top speed for a  $b_y$  decrease of 31.25% was only 1.26 %, meaning that the lowering of corner velocities did not contribute for a significant drop in top speed.

### 3.4. Estimator Sensitivity Analysis

The energy consumption estimation is common between the two simulators. This estimation is done through equation (2) without the angular inertia and hill climb terms. In this section, a sensitivity analysis is done to this estimator seeking to conclude if it is rightly applied to both simulators.

#### 3.4.1 Linear Inertia

For this analysis, the variation of the propulsion force is done through a multiplication factor applied to the linear inertia term of equation (2). The results of the sensitivity analysis of the linear inertia term of the estimator are shown in Figure 11.

#### 3.4.2 Aerodynamic Drag

In the simulation models, higher  $SCX$  values result in lower longitudinal acceleration and subse-

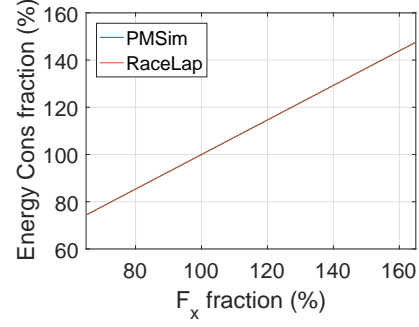


Figure 11: Energy Consumption Estimator sensitivity analysis with  $F_x$  variation in fraction of the default values of Sections 3.1 and 3.2.

quently lower top speeds. These two variables impact the energy consumption through equation (2). Nevertheless,  $SCX$  is also a variable in this equation. This way, the drag coefficient is present in both the simulation models and the estimator. The sensitivity analysis to the aerodynamic term of the energy consumption equation is done to the  $SCX$  in the estimator. The results are plotted in percentage of the nominal energy consumption result in both simulations: 5.62 kWh for RaceLap and 6.62 kWh for PMSim.

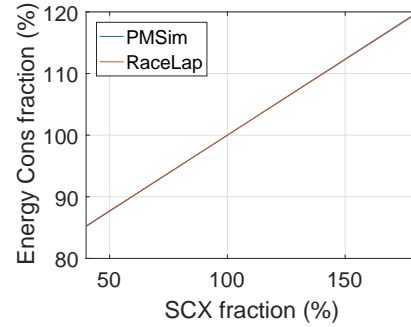


Figure 12: Energy Consumption Estimator sensitivity analysis with drag coefficient variation in fraction of the default values of Sections 3.1 and 3.2.

#### 3.4.3 Rolling Resistance

The tyres rolling resistance ( $f_{rr}$ ), like the aerodynamic drag, contribute to lowering the longitudinal acceleration in the simulation models and is also present in the energy consumption equation (2). Here, a sensitivity analysis is applied to  $f_{rr}$  in the estimator using the outputs from both simulators.

### 4. Conclusions

An energy consumption estimator was successfully implemented in two different lap time simulators with very different vehicle model complexi-

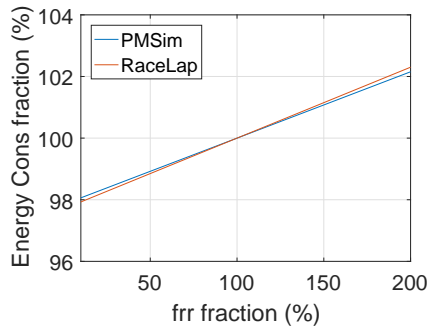


Figure 13: Energy Consumption Estimator sensitivity analysis with rolling resistance coefficient variation in fraction of the default values of Sections 3.1 and 3.2.

ties. The outcome of this work can be applied in the design of the energy storage system of an electric competition vehicle. Results show that the linear inertia of the vehicle is the main contributor of energy loss, followed by the aerodynamic drag and a relatively small contribution of the tyres rolling resistance. The estimator has identical variations when applied to different simulators outputs, working for both a commercial 4-wheel model and a Point-Mass model developed in the scope of this work with about 88% less input parameters.

Modelling the AD03 and the Estoril track in RaceLap resulted in satisfactory simulation results validated by a real test lap. Adjusting the grip level to approximate the hard compound tyres model to the medium compound used in the real car, it was found that increasing the grip factor more than 10% only affects the longitudinal behaviour of the car, inducing in unrealistic simulations.

In the Point-Mass simulation it was found that neither of the aerodynamic coefficients have enough impact in lap time and top speed to be a considerable source of error in the model. The same happens when reducing the longitudinal friction coefficient. On the other hand, the variation of the torque factor applied to the engine torque output significantly impacts the resulting top speed. From this was concluded that the source of longitudinal acceleration that mainly impacts the top speed of the vehicle is the engine propulsion force. Regarding the lateral behaviour of the vehicle, results show that the lateral coefficient of friction has a considerable impact in lap time leading to the conclusion that this is the main source of discrepancies in the Point-Mass model. This agrees with the main difference between the two simulators used in this work being in the lateral acceleration output. Because the lateral coefficient of friction has no significant impact in top speed and the torque factor reduction alone does not impact

enough the lap time, it is concluded that the errors in longitudinal and lateral behaviour are independent of each other.

Because the main source of error in the Point-Mass model comes from the simplification of the tyres model, a recommendation for improving this work is implementing a "bicycle" model. This vehicle model includes a distinction between the front and rear axles of the car and calculates tyre slip angle and vehicle side slip. Knowledge of these angles in each track segment gives the opportunity to implement a full Pacejka tyre model to calculate longitudinal and lateral tyre forces with more precision.

The implementation of simulation tools must always be accompanied by testing for validation purposes.

### Acknowledgements

I want to thank everyone at Adess-AG for the opportunity of developing this work with the team.

### References

- [1] Blake Siegler. *Lap Time Simulation for Race Car Design*. PhD thesis, The University of Leeds, 2002.
- [2] William F. Milliken and Douglas L. Milliken. *Race Car Vehicle Dynamics*, chapter 5.2, pages 126–128. Society of Automotive Engineers, Inc, 1995.
- [3] Tiago Vieira Neves. Development of a numerical model for dynamic handling of competition vehicles. Master's thesis, Instituto Superior Técnico, Universidade Técnica de Lisboa, 2012.
- [4] Philippe Lebeau, Cedric De Cauwer, Joeri Van Mierlo, Cathy Macharis, Wouter Verbeke, and Thierry Coosemans. Conventional, Hybrid, or Electric Vehicles: Which Technology for an Urban Distribution Centre? *Scientific World Journal*, 2015, 2015.
- [5] Cedric De Cauwer, Joeri Van Mierlo, and Thierry Coosemans. Energy consumption prediction for electric vehicles based on real-world data. *Energies*, 8(8):8573–8593, 2015.
- [6] Mohamed El Baghdadi, Laurent De Vroey, Thierry Coosemans, Joeri Van Mierlo, and Rafael Jahn. Electric Vehicle Performance and Consumption Evaluation. *World Electric Vehicle Journal*, 6:30–37, 2013.
- [7] Hans B. Pacejka. *Tyre and Vehicle Dynamics*, chapter 4.3. Elsevier, 2006.
- [8] H.J.C. Luijten C.H.A., Criens; T. ten Dam and T. Rutjes. Building a matlab based formula student simulator. Master's thesis, Technische Universiteit Eindhoven, 2006.
- [9] Gabriel Benjamim Teixeira Rodrigues. Modelação e simulação de um formula student eléctrico. Master's thesis, Instituto Superior Técnico, Universidade Técnica de Lisboa, 2009.